DOI:10.1021/jf103203e

JOURNAL OF AGRICULTURAL AND FOOD CHEMISTRY
ARTICLE

The *Arabidopsis PAP1* Transcription Factor Plays an Important Role in the Enrichment of Phenolic Acids in *Salvia miltiorrhiza*

YUAN ZHANG, YA-PING YAN, AND ZHE-ZHI WANG*

Key Laboratory of the Ministry of Education for Medicinal Resources and Natural Pharmaceutical Chemistry, National Engineering Laboratory for Resource Development of Endangered Crude Drugs in Northwest of China, College of Life Sciences, Shaanxi Normal University, Xi'an, Shaanxi 710062, China

Phenolic acids are health-promoting but low content secondary metabolites in *Salvia miltiorrhiza*. Here, the *Arabidopsis* transcription factor *Production of Anthocyanin Pigment 1* (*AtPAP1*) was expressed in *S. miltiorrhiza* and improved the antioxidant capacity in transgenic plants up to 3-fold. Salvianolic acid B (Sal B) biosynthesis was strongly induced (10-fold higher) in 1 month old transgenic plantlets, a growth stage not normally characterized by significant levels of phenolic acids. This high-Sal B phenotype was stable in roots during vegetative growth, with tissues accumulating approximately 73.27 mg/g of dry weight. Total phenolics, total flavonoids, anthocyanin, and lignin were also significantly enhanced. Consistent with these biological and phytochemical changes, expression of phenolic acid biosynthetic genes was stimulated. Our results demonstrate that *AtPAP1* has an additional, previously unknown, role as a transcriptional activator of phenolic acid biosynthesis in *S. miltiorrhiza*. The results provide a promising strategy for engineering phenolics production in economically significant medicinal plants.

KEYWORDS: *Arabidopsis* PAP1; *Salvia miltiorrhiza* Bunge; phenolic acids; salvianolic acid B; antioxidant activity

INTRODUCTION

Salvia miltiorrhiza Bunge ("danshen" or "tanshen" in Chinese) is a well-known traditional herbal medicine (*1*, *2*). Its active constituents can be divided into two groups: (1) lipid-soluble tanshinones and (2) water-soluble phenolic acids, for example, rosmarinic acid (RA) and salvianolic acid B (Sal B) (*3*). Phenolic compounds protect plants against biotic and abiotic stimuli and play an important role in the treatment of human diseases (*4*). The phenolic acids from *S. miltiorrhiza* have drawn considerable attention in recent years because they are the main components in root water decoction, which is the major form administered to patients in clinical medications in China and Japan (*1*−*4*). Sal B, the predominant bioactive ingredient in that species, is responsible for the treatment of many cardiovascular diseases, especially its significant antioxidant capability and inhibitory effect on matrix metalloproteinase-9 activity (*1*, *5*, *6*). It has been incorporated into numerous finished products, either as single or combined preparations.

All of these reports strongly suggest that the ability to increase the Sal B content in *S. miltiorrhiza* would benefit human health. To enhance the production of tanshinones or phenolic acids in that species, many means have been employed based on hairy root cultures, changes in ploidy as induced by colchicine treatment, or through the use of elicitors or T-DNA activation tagging (*7*−*11*). However, because of high demand (about 80 million kg per year in China), a long growth cycle (2−3 years), and relatively low innate contents, *S. miltiorrhiza* and its phenolics-containing preparations cannot meet the rapidly increasing market needs (*12*). Therefore, biological approaches are required, particularly to elevate Sal B contents. The development of plant metabolic engineering through specific regulation of secondary metabolism is a promising alternative strategy for generating medicinal plants with enhanced health-promoting compounds. In addition, such methods can be used to elucidate the mechanisms that underlie changes in metabolites at the molecular level.

Water-soluble phenolic acids in *S. miltiorrhiza* have similar basic structures, including a series of polymers of caffeic acid modified through sequential oxygenation and coupling reactions (*4*). In plants, these compounds are mainly biosynthesized via a one-branch pathway of core phenylpropanoid metabolism (*10*, *13*, *14*). A biosynthetic pathway has been proposed for RA and Sal B in *S. miltiorrhiza* (**Figure 1**). In addition to the phenolic acid-branched pathway, core phenylpropanoid metabolism is also the upstream pathway for flavonoids (e.g., anthocyanins, flavones, flavonols, and their glycosides) and lignins (i.e., G, S, and H lignin monomers), all of which share the same precursor for phenolic acid biosynthesis (*15*, *16*). Therefore, perturbation of either pathway is not confined to a single branch but induces some redirection of phenylpropanoid metabolism. Generally, overexpression of transcription factors that regulate the expression of genes involved in entire metabolic pathways is an effective tool for engineering high levels of metabolites (*17*). Ectopic expression has been reported for transcription factors that function in different branches of phenylpropanoid metabolism, both in the species of origin and in heterologous species. For example, heterologous expression of *DELILA*

*To whom correspondence should be addressed. Tel: 86-29-85310260. Fax: 86-29-85310546. E-mail: zzwang@snnu.edu.cn.

 Published on Web 11/08/2010

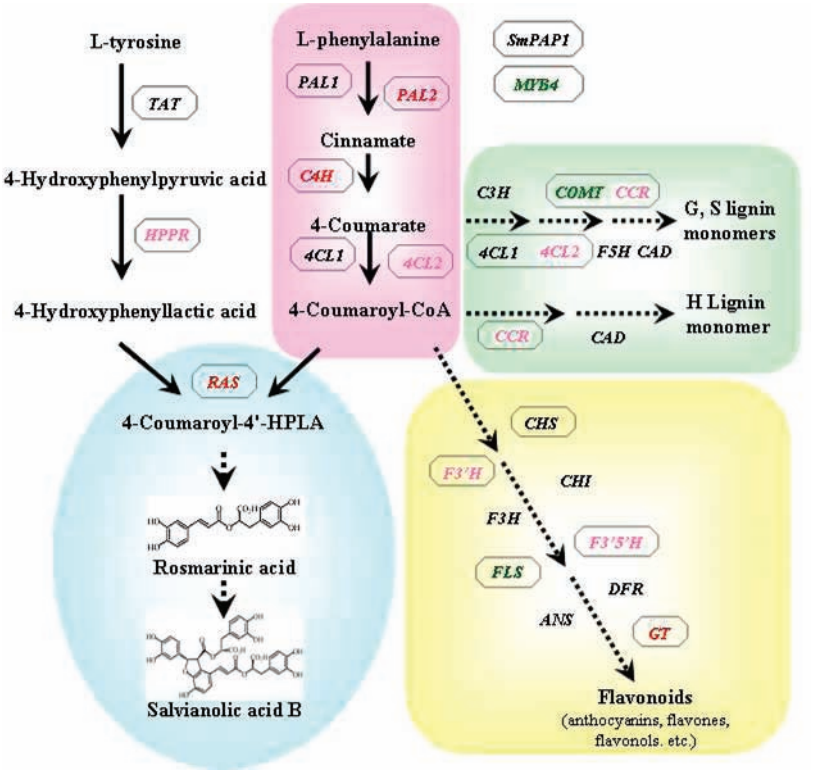

Figure 1. Schematic overview of phenolic biosynthesis pathway in *S. miltiorrhiza*, starting with core phenylpropanoid pathway (pink box) and leading to three major branch pathways: phenolic acid (blue box), flavonoids (yellow box), and lignin (green box). Genes investigated here are in gray frames. They are grouped into four categories based on responsiveness to heterologous *AtPAP1* expression. The first category—*PAL1*, *4CL1*, *TAT*, *CHS*, and *SmPAP1*—showed minimal correlation to *AtPAP1* (gene names in black). The second category (in pink)—*4CL2*, *CCR*, *HPPR*, *F3′H*, and *F3′5′H*—were slightly up-regulated by *AtPAP1*. The third category (in red)—*PAL2*, *C4H*, *RAS*, and *GT*—showed distinct up-regulation. The fourth category (in green)—*COMT*, *FLS*, and *MYB4*—had markedly depressed expression. Abbreviations: *ANS*, anthocyanidin synthase; *CAD*, cinnamyl alcohol dehydrogenase; *CCR*, cinnamoyl-CoA reductase; *C3H*, coumarate 3-hydroxylase; *C4H*, cinnamate 4-hydroxylase; *CHI*, chalcone isomerase; *CHS*, chalcone synthase; *4CL*, hydroxycinnamate-CoA ligase; *COMT*, caffeic acid *O*-methyltransferase; *DFR*, dihydroflavonol 4-reductase; *F3H*, flavanone 3-hydroxylase; *F3′H*, flavonoid 3′-hydroxylase; *F3′5′H*, flavonoid 3′,5′-hydroxylase; *F5H*, ferulate 5-hydroxylase; *FLS*, flavonol synthase; *GT*, glycosyl transferase; *HPPR*, hydroxyphenylpyruvate reductase; *PAL*, phenylalanine ammonia lyase; *PAP1*, production of anthocyanin pigment 1; *RAS*, rosmarinic acid synthase-like; *TAT*, tyrosine aminotransferase.

(*DEL*) and *ROSEA1* (*ROS1*), encoding bHLH and MYB transcription factors from snapdragon (*Antirrhinum majus*), improved the amounts of anthocyanins in transgenic tomato fruit and enhanced their antioxidant capacity (*17*). Overexpression of *LC* and *C1*, encoding two transcription factors that control anthocyanin biosynthesis in maize, led to increased levels of flavonols in tomato (*18*). *Production of Anthocyanin Pigmentation 1* (*AtPAP1*), encoding a MYB transcription factor in *Arabidopsis thaliana*, can effectively induce anthocyanin production not only in *Arabidopsis* but also in tobacco and canola (*19*−*21*), thereby demonstrating its conserved characteristics among species. Therefore, we believe that the earlier research on the manipulation of the phenylpropanoid pathway in heterologous species provides an approach that we can use to regulate phenolic acid biosynthesis in *S. miltiorrhiza*.

Here, the *Arabidopsis PAP1* transcription factor was constitutively expressed under the control of the cauliflower mosaic virus (CaMV) 35S promoter in *S. miltiorrhiza*. Contents of individual phenolic acids, total phenolics, total flavonoids, anthocyanins, and lignins were evaluated in control and transgenic plants, and the antioxidant capacity of root extracts was determined. In addition, we monitored the expression of endogenous genes and regulators in the phenylpropanoid pathway to understand the molecular mechanisms that underlie these metabolite alterations. Our objective was to present a tool that can be utilized with *AtPAP1* to improve the potential of *S. miltiorrhiza* to produce health-promoting antioxidant phenolic acids and provide protection against redox-related diseases. To our knowledge, this is the first report of phenolic acid accumulations in transgenic medicinal plants.

MATERIALS AND METHODS

Experimental Materials. The seeds of *S. miltiorrhiza* were collected from Shangluo, Shaanxi Province of China. The plants were grown in pots in the greenhouse of our laboratory at 25 °C with a 16 h light period and relative air humidity of 60%. A voucher specimen (#DS080916) was identified by Professor Yi Ren and deposited in the Key Laboratory of the Ministry of Education for Medicinal Resources and Natural Pharmaceutical Chemistry, China. Root cutting of the certified *S. miltiorrhiza* was used for generating a stable asexual reproduction. The transformation procedure was developed using leaf explants from the stable asexual propagation line of *S. miltiorrhiza*. All chemicals were obtained from Sigma Chemical Co. (St. Louis, MO). Solvents were high-performance liquid chromatography (HPLC) grade. Standards of RA and Sal B were purchased from the National Institute for the Control of Pharmaceutical and Biological Products (Beijing, China). All standards were prepared as stock solutions in methanol and were stored in the dark at −18 °C. Primer pairs are listed in Table S1 in the Supporting Information. Sterile plantlets of *S. miltiorrhiza* Bunge were cultured on MS basal medium as described by Yan and Wang (*22*).

Vector Construction and Plant Transformation. The full-length cDNA coding sequence for *Arabidopsis PAP1*(AT1G56650) (NCBI reference sequence NM_104541.3) was amplified from leaf cDNA using gene-specific primers *AtPAP1*-F and *AtPAP1*-R, which contain *Bgl*II or *BstE*II restriction sites, respectively. Polymerase chain reaction (PCR) products were cloned into a pGEM T-easy cloning vector and sequenced by Sangon Biological Engineering Technology & Services Co., Ltd.

(Shanghai, China). The *AtPAP1* cDNA fragment was inserted, using *Bgl*II/*Bst*EII sites, into the binary vector pCAMBIA1302, where its expression was driven by the CaMV 35S promoter. This generated the *AtPAP1* overexpression vector PAP1-OE (Figure S1 in the Supporting Information). Plasmid PAP1-OE was mobilized into *Agrobacterium tumefaciens* EHA105 by electroporation. Resistant colonies were verified by PCR amplification and used for transformation experiments. Leaf explants from *S. miltiorrhiza* were used to generate transgenic plants with PAP1-OE via *A. tumefaciens*-mediated transformation (*22*). One month old plantlets were used for PCR screening, expression analysis, and preliminary measurements of phenolic acid contents. Positive plants were then transplanted into soil and cultivated in the greenhouse for further examination.

Nucleic Acid Extraction and RT-PCR. Genomic DNA was obtained from transgenic and wild-type plants by a modified CTAB method. Total RNA was isolated with Trizol reagent (BioFlux, China). The quality and the concentration of genomic DNA and RNA were determined by 1.0% agarose gel electrophoresis and spectrophotometry (SHIMADZU UV-2450, Japan). Total RNA was used to produce cDNA with the oligo$(dT)_{18}$ primer and a RevertAID First Strand cDNA Synthesis Kit (MBI, United States) according to the manufacturer's instructions.

PCR Detection of Transgenic Plants. A pair of gene-specific primers (*AtPAP1*-F and *AtPAP1*-R) was used to amplify a 747 bp fragment from genomic DNA of transgenic and wild-type plants. PCR reactions were carried out in a PTC-200 thermocycler (Bio-Rad, United States) in a 20 μL solution containing 0.05 μL of DNA, 2 μL of 10 × PCR reaction buffer, 2 μL of dNTP (2.5 mM), 2 μL of Mg^{2+} (2.5 mM), 0.5 μM concentration of each primer, and 0.5 U of rTaq DNA polymerase (Takara, Japan). The mixtures were treated at 94 °C for 5 min, then subjected to 35 cycles of amplification (94 °C for 30 s, 55 °C for 30 s, and 72 °C for 50 s), followed by a final elongation of 10 min at 72 °C. The overexpression vector PAP1-OE served as the positive control, and genomic DNA from wild-type plants served as the negative control. Amplified products were electrophoresed on a 1.0% agarose gel.

RT-PCR Analysis. To estimate transcript levels of exogenous *AtPAP1* in different samples, we used primers *AtPAP1*-S-F and *AtPAP1*-S-R for amplification (Table S1 in the Supporting Information). PCR conditions were 94 °C for 5 min; then 33 cycles of 94 °C for 30 s, 51 °C for 30 s, and 72 °C for 25 s; followed by 72 °C for 10 min. Equal loading of each amplified gene sequence was determined using the internal control *SmEF1*-α, which is orthologous to *Arabidopsis EF1*-α. For *SmEF1*-α amplification, essentially the same conditions were used except that annealing occurred at 55 °C and the number of cycles was reduced to 25.

Real-Time Quantitative PCR Measurements. Quantitative PCR was carried out on a iQ5 thermocycler (Bio-Rad) in a 20 μL final volume comprising appropriately diluted cDNA, 0.2 μM concentration of each primer, and 10 μL of 2 × Q-PCR Mix that contained SYBR Green I (Takara). The standard thermal profile included 1 min of predenaturation at 94 °C (1 cycle) and 35 cycles of 10 s denaturation at 94 °C, 20 s annealing at 60 °C, and 15 s of collection fluorescence at 82 °C. Melting curve analysis was performed from 50 to 95 °C using Dissociation Curve software (BioRad iQ5 Optical System Software, United States). A fragment of the *ubiquitin* gene was amplified as an internal control to calibrate relative expression. Reactions that replaced the cDNA template with nuclease-free water were run with each primer pair as a blank control. Quantification consisted of at least three independent replicates. All PCR reactions were 95−100% efficient. Expression was evaluated based on publicly available gene sequences (*23*, *24*) and quantified according to the comparative C*T* method. Gene-specific primers for quantitative PCR are listed in Table S1 in the Supporting Information.

Extraction of Soluble Phenolic Compounds. The plantlets (including roots, stems, and leaves) or roots harvested from greenhouse-grown plants at six developmental stages were air-dried at 20 ± 2 °C. Root samples were identified according to time of collection, that is, D45 (45 days after planting), D115, D130, D165, D195, and D225. Dried samples were ground to a fine powder in a mechanical grinder with a 2 mm diameter mesh. Approximately 100 mg of tissue was extracted with 500 μL of 75% methanol under sonication for 20 min and then centrifuged at 12000*g* for 6 min. The supernatant was collected, and the residual pellet was re-extracted two times with 500 μL of solvent. All supernatants were combined as a total extract for the determination of phenolic compounds. Extraction was done in triplicate.

HPLC Analysis of Phenolic Compounds. Extracts were analyzed on a SHIMADZU C_{18} column (5 μm, 150 mm × 4.6 mm) connected to an LC-2010A HPLC system equipped with an SPD-M10 V photodiode array (PDA) detector and LC-Solution software (SHIMADZU, Kyoto, Japan). The mobile phase comprised 0.4% acetic acid in water (A), acetonitrile (B), and methanol (C). The solvent gradient was as follows: 0−5 min, A 95 to 90% and B 5−10% B; 5−25 min, A 90 to 67%, B 10−30%, and C 0−3%; 25−40 min, A 67 to 60%, B 30−35%, and C 3−5%. Conditions included a flow rate of 1.0 mL/min, column temperature of 30 °C, injection with 20 μL of sample, and PDA detector wavelengths ranging from 200 to 800 nm, with samples measured at 280 nm. Samples and mobile phases were put through a 0.22 μm filter before injection. Major peaks from these extracts were identified by comparison to known retention times, and UV spectra of authentic standards were assessed under identical conditions. These values were further verified by analyzing their fragmentation patterns via LC/MS/MS (data not shown).

Lignin Analysis. Air-dried stems from 6 month old plants (approximately five per sample) were ground sufficiently to pass through a 2 mm diameter mesh and then exhaustively extracted for 24 h with acetone in a Soxhlet apparatus. Extractive-free material was used for all further analyses. Contents of Klason lignin and acid-soluble lignin were measured according to the protocol of Ma (*25*), and 25 mg of extractive-free stem tissue was used to determine the lignin monomer composition by a streamlined thioacidolysis procedure (*26*). The main *p*-hydroxyphenyl (H), guaiacyl (G), and syringyl (S) lignin monomers were analyzed via gas chromatography−mass spectrometry (GC-MS). Qualitative and quantitative analyses of individual lignin monomers, per their trimethylsilylated derivatives, were performed from specific ion chromatograms reconstructed (at m/z 239 for the H monomers, 269 for G, and 299 for S) after making an appropriate calibration relative to the tetracosane internal standard (*27*).

Determination of Total Phenolic, Total Flavonoid, and Anthocyanin Contents. One gram samples of powder from transgenic or wild-type plants were extracted with 30 mL of acidified (0.3% HCl, v/v) methanol for 24 h at 4 °C, with moderate shaking. Afterward, they were centrifuged at 4 °C for 30 min at 5000*g*. The pellet was washed with 2 × 15 mL of solvent. Supernatants were combined as a total extract and stored at 4 °C. We have previously reported a detailed methodology for determining total phenolics and flavonoids (*28*). Quantification of anthocyanins was performed according to the protocols of Mano et al. (*29*).

Total Antioxidant Activities. Antioxidant activities for MeOH extracts from transgenic and wild-type roots (D150) were measured for TEAC (trolox equivalent antioxidant capacity). This assay is based on the ability of antioxidant molecules to quench the long-lived ABTS (2,2′-azinobis 3-ethylbenzthiazoline-6-sulfonate; Sigma-Aldrich) radical cation, a blue-green chromophore with characteristic absorption at 734 nm. That finding was then compared with one for trolox (6-hydroxy-2.5,7,8-tetramethylchroman-2-carboxylic acid; Fluka), a water-soluble vitamin E analogue. Results were expressed as TEAC in mM of trolox per gram of dry weight (DW).

Statistical Analysis. One-way analysis of variance (ANOVA) and Tukey's multiple comparisons were performed with SPSS (version 13.0). Differences between means at the 5% confidence level were considered significant. Correlation coefficients (r) to determine the relationships among variables were calculated using the Bivariate correlation statistical function.

RESULTS

Generation of Transgenic *S. miltiorrhiza* Plants. Following *Agrobacterium*-mediated transformation, 13 hygromycin-resistant plantlets regenerated from calli and showing strong growth were preselected by PCR. Molecular analysis indicated that the exogenous *AtPAP1* was stably integrated into the *S. miltiorrhiza* genome. A total of 11 transgenic lines exhibited the expected signal for the *AtPAP1* transgene, which was not amplified in the wild-type sample (**Figure 2A**). Expression of the transgene was verified by RT-PCR (for whole plants) and real-time quantitative PCR (for leaves, stems, and roots). Transgenic lines PAP1-1, -2, -10,

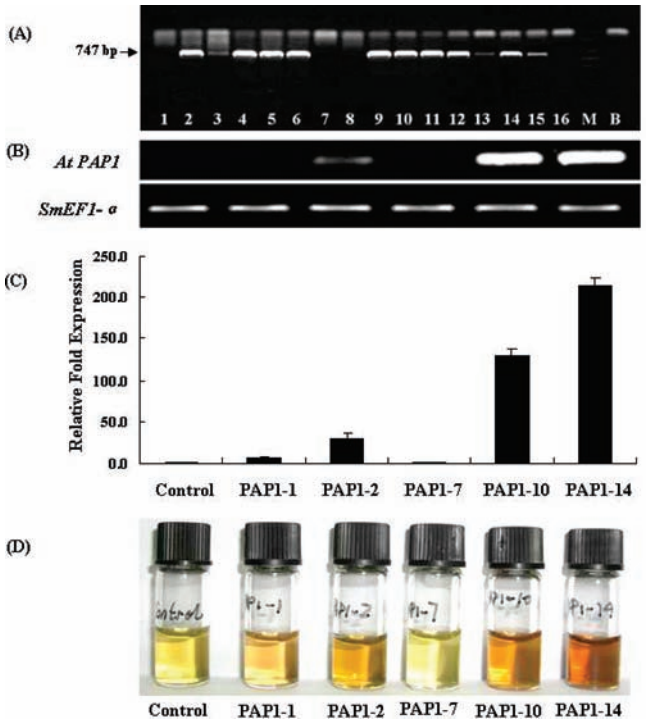

Figure 2. Expression of *AtPAP1* in overexpressing transgenic lines. (**A**) PCR detection. M, DL2,000 DNA marker; band sizes from top: 100, 250, 500, 750, 1000, and 2000 bp. Lane 1, control; lane 2, positive control (*AtPAP1* overexpression vector PAP1-OE); lanes 3−16, different transgenic lines; b, no template control. (**B**) Semiquantitative RT-PCR results. (**C**) Real-time quantitative PCR analysis; all data are means of three replicates, with error bars indicating SD. (**D**) Visible signs of soluble phenolic extracts in transgenic lines and control. PAP1-1, -2, -7, -10, and -14: randomly selected hygromycin-resistant and PCR-positive transgenic lines.

and -14 had obvious overexpression of *AtPAP1* (**Figure 2B**,**C**). The highest expression (200-fold greater than the wild-type control) was detected in line PAP1-14. Relative transcript levels from other overexpressing lines ranged from 6.8- to 128.6-fold higher. However, line PAP1-7 showed no significantly enhanced expression even though PCR analysis showed that it contained the *AtPAP1* cassette. Two lines (PAP1-10 and PAP1-14) with comparatively higher accumulations of transcripts were selected for further investigation. Our controls were wild-type plants or those transformed only with binary vector pCAMBIA1302. Although the CaMV 35S promoter was used to drive the transgene, *AtPAP1* expression varied among the organs of PAP1-10 and PAP1-14 plants, with transcripts being highest in the leaves, while those in the stems and roots were similar to each other and approximately 2-fold lower than in leaf tissue (Figure S2 in the Supporting Information).

Transgenic plants maintained in a greenhouse were morphologically indistinguishable from nontransformed control plants. Moreover, their rates of germination and growth were the same during the vegetative phase (data not shown), indicating that *AtPAP1* expression, even at an elevated level, did not affect normal development of *S. miltiorrhiza*. However, when mature leaves from different lines were extracted (with phosphate buffer, pH 7.0) and clarified (by centrifugation and filtration), a vast difference was seen in the filtrates, which were brown from the *AtPAP1* expressing lines and translucent pale-yellow from the control (**Figure 2D**). This suggested that the transgenic plants contained more phenolic compounds than the control (i.e., the brown color was due to a mixture of oxidized phenolics).

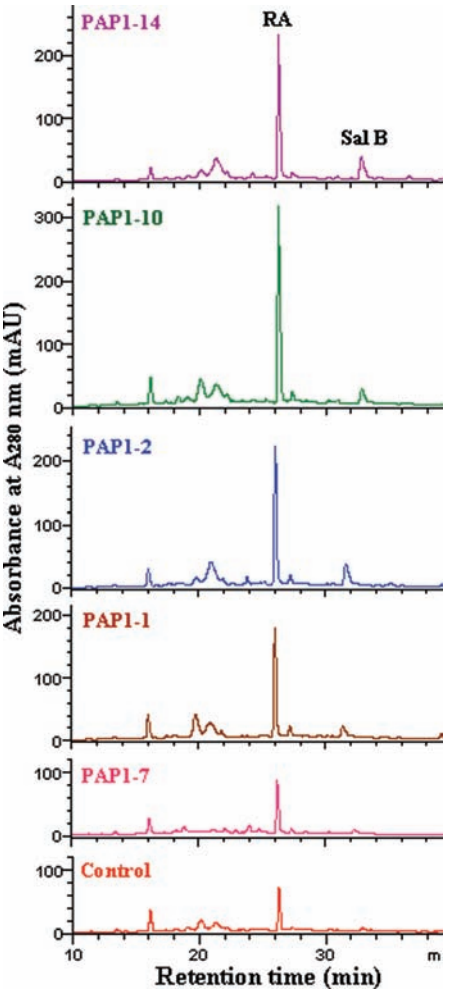

Figure 3. Representative HPLC chromatograms of 1 month old *S. miltiorrhiza* lines. Control: wild-type; PAP1-1, -2, -7, -10, and -14: randomly selected positive transgenic lines.

Global Comparison of Phenolics Profiles. To further characterize how phenolic metabolism is modified in *AtPAP1* overexpressing plants, phenolic acids were extracted and subjected to HPLC separation. There, RA and its dimer Sal B were major components in 1 month old plantlets (including roots, stems, and leaves), with retention times of 26.3 and 32.8 min, respectively (**Figure 3**). The highest contents were found in line PAP1-14, with mean levels of up to 15.00 ± 0.36 mg/g DW RA and 5.09 ± 1.04 mg/g DW Sal B, followed by line PAP1-10 (Table S2 in the Supporting Information). For wild-type, RA and Sal B contents were 1.44 ± 0.18 and 0.82 ± 0.15 mg/g DW, respectively, approximately 10.42- and 6.21-fold lower than in line PAP1-14. HPLC analysis of extracts from whole plants and individual organs (roots, stems, and leaves) revealed similar patterns of increases in the amounts of major phenolic acids, with RA and Sal B being distributed throughout each plant (Figure S3 in the Supporting Information). Thus, we suggest that any changes in the secondary metabolic pathways for phenolic compounds may be important for their biosynthesis. Comparative HPLC data showed that higher levels of RA and Sal B accumulated in all tissues from lines PAP1-10/14 relative to the wild type (Figure S3 in the Supporting Information).

As sink organs, roots accumulate more phenolic acids during plant development, such that dry roots are a valuable medicinal source. To determine whether the high-Sal B phenotype was stable during vegetative growth, we examined in detail the roots

from PAP1-14 and wild-type plants at six growth stages under greenhouse conditions. The Sal B content varied over time. For example, levels gradually increased from 45 to 225 days after planting, and the maximum accumulation occurred at day 165 for both PAP1-14 and wild-type roots (**Figure 4**). Although this pattern was similar between the two genotypes, PAP1-14 roots had persistently higher contents of Sal B over our test period (by 1.96−2.25-fold). After 165 days, the roots of line PAP1-14 contained approximately 73.27 ± 1.68 mg/g DW Sal B, which represented an approximately 2-fold greater accumulation than in wild type (Table S3 in the Supporting Information). RA contents also increased to varying degrees (Table S3 in the Supporting Information), but no significant differences were observed for lipid-soluble tanshinones (data not shown). This new high-Sal B *S. miltiorrhiz* a could be crossed to lines enhanced with tanshinones and then examined for potential as high-quality medicinal materials.

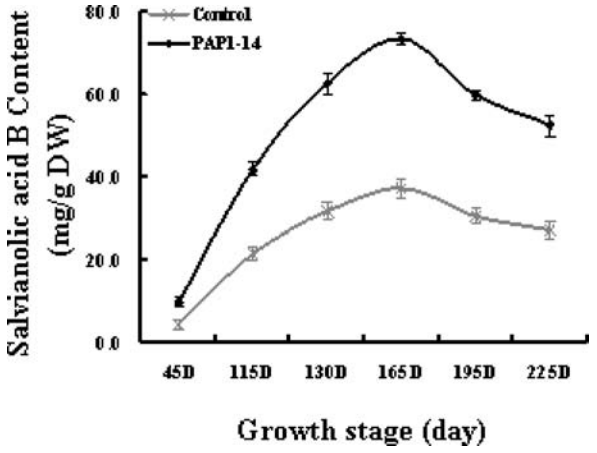

Figure 4. Variation in content of Sal B among roots of PAP1-14 and control lines at different growth stages. Day 1: March 26, 2009 (i.e., early Spring in Xi'an, China). All data are means of three replicates, with error bars indicating SD.

Phenolic, Flavonoid, Anthocyanin, and Lignin Contents in Transgenic Plants. Our results above demonstrated that the introduction of *AtPAP1* modified accumulation of nonflavonoid phenolic acids (RA and Sal B). To evaluate whether the up-regulation could cause the activation of the phenylpropanoid pathway and provide substrates for the biosynthesis of other types of end products, we also performed global assays for phenolics, flavonoids (including anthocyanin), and lignin contents. Here, total phenolics and total flavonoids accumulated at higher levels in the roots of PAP1-10/14 lines as compared with the control. Differences were significant and corresponded to 1.43- and 1.70-fold increases in total phenolics content of PAP1-10/14 roots and 1.27- and 1.57-fold increases in total flavonoid contents (**Figure 5A**,**B**). Although all transgenic plants were phenotypically similar to the wild type, we calculated a slightly, but significantly, higher anthocyanin content in root extracts from line PAP1-14 (**Figure 5C**).

The content and composition of lignin also were examined because it is derived from the same precursors as phenolics and flavonoids. After 6 months of growth, air-dried stems from transgenic and wild-type plants were evaluated for total cell wall composition, including acid-soluble and acid-insoluble lignins (**Table 1**). In PAP1-10 and PAP1-14 plants, klason lignin (acid-insoluble) contents were approximately 1.21- and 1.29-fold higher than in the wild type. This increase was found for both lignin

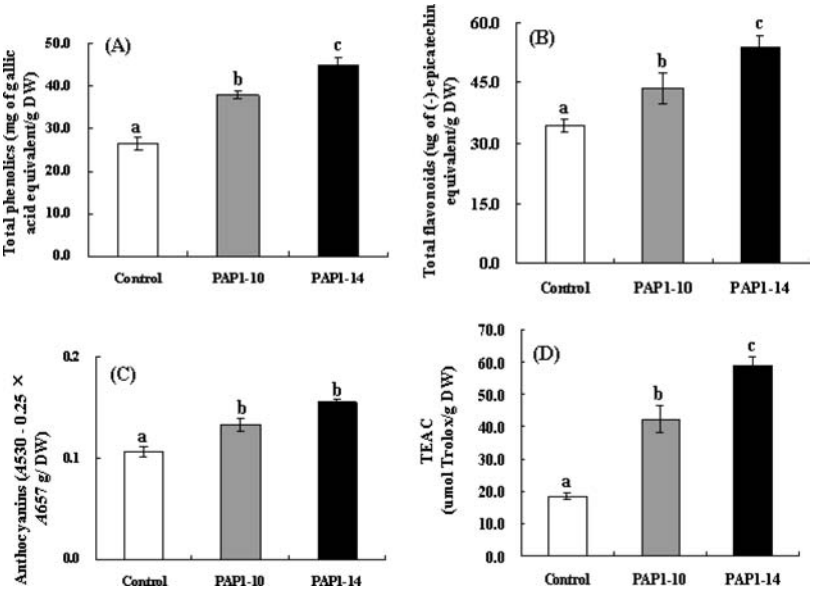

Figure 5. Total phenolic (**A**), total flavonoid (**B**), and anthocyanin (**C**) contents and TEAC (**D**) in root extracts from control and transgenic lines. Values followed by same letter within a column are not significantly different ($p > 0.05$). All data are means of three replicates, with error bars indicating SD.

Table 1. Lignin Content and Composition within Mature Stems from Control and Transgenic Lines[a]

	lignin (mg/g DW)				monomer yield (μmol/g DW)			
line	acid-soluble lignin	Klason lignin	total lignin	H lignin	G lignin	S lignin	S/G ratio	total yield of (H + G + S) monomers
control	0.12 ± 0.01 a[b]	155.07 ± 10.46 a	155.19 ± 5.22 a	74.29 ± 3.34 a	2196.83 ± 134.33 a	1666.50 ± 100.43 a	0.76	3937.62 ± 75.12 a
PAP1-10	0.17 ± 0.03 b	186.88 ± 12.22 b	187.05 ± 6.06 b	68.31 ± 10.20 a	2612.43 ± 218.02 b	3809.24 ± 486.67 b	1.46	6489.98 ± 236.17 b
PAP1-14	0.18 ± 0.02 b	200.80 ± 11.66 c	200.97 ± 5.64 c	77.63 ± 12.20 a	4542.23 ± 299.24 c	3004.91 ± 197.73 c	0.66	7624.77 ± 168.71 c

[a] Triplicate samples were analyzed for each line. Data are means ± SDs. [b] Column-wise values not followed by the same letter do not differ significantly ($p > 0.05$).

fractions. We also used thioacidolysis to study the impact of *AtPAP1* overexpression on lignin structure. Consistent with total lignin contents, the yield and relative frequency of the G and S thioacidolysis monomers released by stems from line PAP1-14 were significantly more elevated than in control stems, but their S/G ratios varied little (**Table 1** and Figure S4 in the Supporting Information). The low but nevertheless detectable amount of H lignin units in PAP1-14 stems did not differ significantly from the wild type ($p > 0.05$). Although the higher lignin content indicated that *AtPAP1* heterologous expression influences stem lignification, no appreciable phenotypic difference was observed. Therefore, overexpression of *AtPAP1* possibly directed flux into different branches of the phenylpropanoid pathway, resulting in enhanced accumulation of phenolic acids, flavonoids, and lignins in transgenic *S. miltiorrhiza*.

Antioxidant Activities. To investigate the physiological significance of an increase in Sal B levels, we measured TEAC in transgenic and control *S. miltiorrhiza*. The activity was 3.2-fold higher in line PAP1-14 root extracts (**Figure 5D**). Although the increase in antioxidant activity from line PAP1-10 was less pronounced, it was still significantly higher (2.3-fold) than in wild type. Therefore, they could contribute to antioxidant sources in the human diet and might, as health foods, be more widely adopted in preventive medicine strategies by healthy consumers than are current antioxidant supplements.

Because these antioxidant results were very similar to the trend for phenolic compounds, we examined any possible relationship between those two traits. Here, antioxidant activity was significantly correlated with total phenolics ($r = 0.9996$, $p < 0.05$), total flavonoids ($r = 0.9893$, $p < 0.05$), anthocyanins ($r = 0.9986$, $p < 0.05$), and total lignin ($r = 0.9934$, $p < 0.05$). Sal B accumulation also showed a positive correlation with $ABTS^{+}$ radical scavenging activity ($r = 0.9934$, $p < 0.05$). However, antioxidant activity did not correlate with RA ($r = 0.5407$, $p > 0.05$).

Effect of *AtPAP1* on the Expression of Phenolic Pathway Genes. To determine the mechanisms that underlie these phenotypic changes in Sal B content, we examined transcript levels of 15 key structural genes and two regulatory genes in the phenolic biosynthesis pathway of transgenic *S. miltiorrhiza*. Relative to expression in wild type, the PAP1-14 plants showed marked differences in expression of genes in the core phenylpropanoid pathway as well as in the specific branch pathways (**Figure 6**). These genes could be grouped into four categories based on their responsiveness to *AtPAP1*. Those in the first category—*SmPAL1*, *Sm4CL1*, *SmTAT*, *SmCHS*, and *SmPAP1*—were not strongly correlated with heterologous *AtPAP1* expression (change in expression only 1.20−1.39-fold higher), and their transcripts were at levels similar to those in wild type. The second category—*Sm4CL2*, *SmCCR*, *SmHPPR*, *SmF3′H*, and *SmF3′5′H*—showed slight up-regulation (by 1.68−2.46-fold). The effect of constitutive *AtPAP1* expression was more pronounced for members of the third category—*SmPAL2*, *SmC4H*, *SmRAS*, and *SmGT*—where transcripts were distinctly increased (28.06-fold) for *SmRAS* and, to a lesser extent, for *SmGT* (3.25−7.67-fold). Expression was markedly depressed (9−68% decline) for members of the fourth category, that is, *SmCOMT*, *SmFLS*, and *SmMYB4*. These data show that almost all of the genes encoding enzymes required for Sal B biosynthesis (*SmPAL2*, *SmC4H*, *Sm4CL2*, *SmHPPR*, and *SmRAS*) were very responsive to *AtPAP1*, with the alteration of *SmRAS* being most marked.

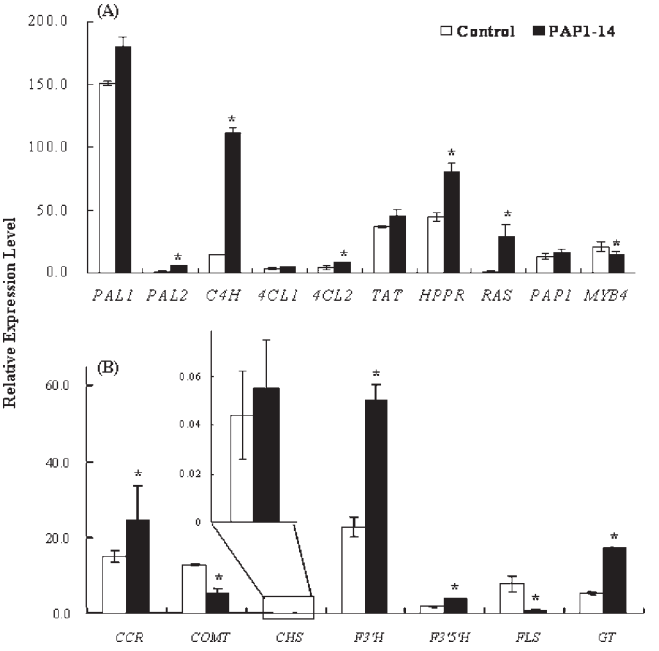

Figure 6. Relative expression levels of phenolic biosynthetic genes in control and PAP1-14 transgenic lines, including those from pathways for phenolic acids (**A**) and flavonoids and lignins (**B**). Regions within black frames are enlarged in *CHS*. All data are means of three independent replicates, with error bars indicating SD. The asterisk indicates the significant difference ($p < 0.05$) between control and PAP1-14 lines.

DISCUSSION

We think that enhanced production of phenolic compounds in transgenic *S. miltiorrhiza* is the primary consequence of heterologous expression of *AtPAP1*, encoding a MYB type regulator. First, Sal B biosynthesis is strongly induced (approximately 10-fold over the control) in very young plantlets (1 month old), a growth stage that normally lacks significant levels of any phenolic acids. Second, the accumulation patterns for major phenolic acids among transgenic roots, stems, and leaves are very similar due to the wide expression domains of the CaMV 35S promoter. Third, the high-Sal B phenotype is stable during different developmental stages in the roots. Fourth, levels of RA and Sal B in different transgenic lines correlated well with quantities of *AtPAP1* transcripts, suggesting that the cellular concentration of AtPAP1 is important for such a phenotypic change.

Although *AtPAP1* offers the potential to enhance anthocyanin and lignin biosynthesis (*19*−*21*), its role may vary among plant species and may be more specific to phenolic acid biosynthesis in *S. miltiorrhiza*. The function of *AtPAP1* on phenolic acid production (especially Sal B) has not been previously reported. The differences were possibly due to the efficacy of inducing phenylpropanoid-derived end products and their target gene specificity. Omoto et al. (*30*) measured Sal B and RA contents in the roots of plants from 26 species within Lamiaceae and found Sal B only in *S. miltiorrhiza*, indicating that this species is unique in its high accumulation of that compound. Therefore, we propose that the potential biosynthetic route leading to Sal B is also particularly active in *S. miltiorrhiza*. Using combined molecular and genetics approaches, we have demonstrated that *AtPAP1* serves as a transcriptional activator of late phenolic acid biosynthesis. This suggests that engineering strategies for phytonutrients should involve research into the specificity of proteins from different species to determine those most effective for achieving metabolic objectives.

We partitioned the phenolic biosynthetic pathway in transgenic *S. miltiorrhiza* toward core phenylpropanoids, phenolic acids, flavonoids, and lignin by combining metabolic information with gene expression data. Sal B accumulated at high levels in that

species for several reasons. First, *AtPAP1* activated a broader spectrum of genes in the core pathway. *PAL* and *C4H* transcript levels were increased substantially. PAL is the first enzyme in that pathway and is also the branch point between primary and secondary metabolism. C4H is the second key enzyme in the general phenylpropanoid pathway (*24*) and, along with PAL, determines flux through phenylpropanoid metabolism. Both participate in many physiological processes involving lignification, flavonoid synthesis, and pathogen defense (*24*). Therefore, the effects of *AtPAP1* overexpression on *PAL* and *C4H* expression may explain the enrichment of phenolic compounds in our transgenic lines. Second, *AtPAP1* induced RAS hypertranscription (approximately 20-fold higher than in the control lines). RAS catalyzes the condensation reaction of 4-hydroxyphenyllactic acid and 4-coumaroyl-CoA. They are important precursors to the formation of 4-coumaroyl-4′-hydroxyphenyllactic acid, which is further transformed into RA. Importantly, RAS is an entry point from the core phenylpropanoid pathway to the phenolic acid branch pathway; here, its transcript level determined the rate of RA and Sal B synthesis. Because RAS may regulate the flux into phenolic acid metabolism by *S. miltiorrhiza*, the ability of *AtPAP1* to induce this gene may also contribute to those high levels of Sal B accumulation. Third, *SmPAP1* was apparently unaffected by *AtPAP1* overexpression. AtPAP1 showed more than 70% similarity to the endogenous PAP1 in *S. miltiorrhiza* (SmPAP1), based on homology analysis by Blast X searches in the NCBI database (http://www.ncbi.nlm.nih.gov/BLAST/). In contrast, *SmMYB4*, a negative regulator of *SmC4H* in the phenylpropanoid pathway of *S. miltiorrhiza*, was slightly but significantly repressed in line PAP1-14 relative to its level in wild type, possibly causing *C4H* expression to increase. Fourth, transcripts of *SmF3′H* and *SmF3′5′H*, two genes active in flavonoid biosynthesis, were strongly up-regulated. However, SmCHS, the entry point enzyme into that branch pathway, was not typically induced. These results provide support that the main effect of *AtPAP1* overexpression is the activation of gene expression within the phenolic acid biosynthetic pathway.

Our findings demonstrate that *Arabidopsis PAP1* is effective in enriching the formation of health-promoting phenolic acids, especially Sal B, in *S. miltiorrhiza*, and the transgenic *S. miltiorrhiza* is sufficient for improving in vitro antioxidant activity. As a fundamental research, this study has now revealed that *AtPAP1* has an additional, previously unknown, role as a transcriptional activator of phenolic acid biosynthesis in *S. miltiorrhiza*. This new information enhances our understanding of the transcriptional regulation of phenolic acid biosynthesis. In terms of human nutrition and health, we established a new and high-Sal B lines could be tested as high-quality medicinal sources for the treatment of chronic cardiovascular and cerebrovascular diseases. Moreover, because the use of specific transcription factors would eliminate time-consuming procedures for obtaining knowledge about all of the enzymatic steps within a poorly characterized biosynthetic pathway, our results may provide new clues and potential opportunities for engineering phenolic production in economically significant medicinal plants.

ABBREVIATIONS USED

ABTS, 2,2′-azinobis 3-ethylbenzthiazoline-6-sulfonate; CaMV, cauliflower mosaic virus; CCR, cinnamoyl-CoA reductase; C4H, cinnamate 4-hydroxylase; CHS, chalcone synthase; 4CL, hydroxycinnamate-CoA ligase; COMT, caffeic acid *O*-methyltransferase; DW, dry weight; EF1α, elongation factor 1-α; F3′H, flavonoid 3′-hydroxylase; F3′5′H, flavonoid 3′, 5′-hydroxylase; FLS, flavonol synthase; GT, glycosyl transferase; HPPR, hydroxyphenylpyruvate reductase; PAL, phenylalanine ammonia lyase; PAP1, production of anthocyanin pigment 1; RA, rosmarinic acid; RAS, rosmarinic acid synthase-like; Sal B, salvianolic acid B; TAT, tyrosine aminotransferase; TEAC, trolox equivalent antioxidant capacity; Ub, ubiquitin.

Supporting Information Available: Primers used in experimental procedures (Table S1), contents of RA and Sal B in lines of 1 month old *S. miltiorrhiza* (Table S2), variations in content of RA and Sal B from roots of PAP1-14 and control lines at different growth stages (Table S3), schematic diagram of *AtPAP1* overexpression vector PAP1-OE (Figure S1), expression of *AtPAP1* in different organs from transgenic lines (Figure S2), representative HPLC chromatograms of roots, stems, and leaves from 3 month old plantlets of PAP1-10, -14, and control lines (Figure S3), and typical GC/MS chromatography showing thioacidolysis products from lignin samples of transgenic and control lines (Figure S4). This material is available free of charge via the Internet at http://pubs.acs.org.

LITERATURE CITED

(1) Wang, X.; Morris-Natschke, S. L.; Lee, K. H. New developments in the chemistry and bic of the bioactive constituents of Tanshen. *Med. Res. Rev.* **2007**, *27*, 133−138.

(2) Li, Y. G.; Song, L.; Liu, M.; Hu, Z. B.; Wang, Z. T. Advancement in analysis of *Salviae miltiorrhizae* Radix et Rhizoma (Danshen). *J. Chromatogr. A* **2009**, *1216*, 1941−1953.

(3) Zhou, L.; Zuo, Z.; Chow, M. S. Danshen: An overview of its chemistry, pharmacology, macokinetics, and clinical use. *J. Clin. Pharmacol.* **2005**, *45*, 1345−1359.

(4) Lu, Y.; Foo, L. Y. Polyphenolics of Salvia—A review. *Phytochemistry* **2002**, *59*, 117−140.

(5) Zhao, G. R.; Zhang, H. M.; Ye, T. X.; Xiang, Z. J.; Yuan, Y J.; Guo, Z. X.; Zhao, L. B. Characterization of the radical scavenging and antioxidant activities of danshensu and salviai acid B. *Food Chem. Toxicol.* **2008**, *46*, 73−81.

(6) Jiang, B.; Chen, J.; Xu, L.; Gao, Z.; Deng, Y; Wang, Y; Xu, R; Shen, X.; Guo, D. A. Salvianolic acid B functioned as a competitive inhibitor of matrix metalloproteinase-9 efficiently prevented cardiac remodeling. *BMC Pharmacol.* **2010**, *10*, 1−10.

(7) Yan, Q.; Hu, Z.; Tan, R. X.; Wu, J. Efficient production and recovery of diterpenoid shinones in *Salvia miltiorrhiza* hairy root cultures with in situ adsorption, elicitation semi-continuous operation. *J. Biotechnol.* **2005**, *119*, A16−A2A.

(8) Gao, S.; Zhu, D.; Cai, Z.; Xu, D. Autotetraploid plants from colchicine-treated bud culture of *Salvia miltiorrhiza* Bge. *Plant Cell, Tissue Organ Cult.* **1996**, *47*, 73−77.

(9) Y., X.; Gao, S. H.; Di, P.; Chen, J. R.; Chen, W. S.; Zhang, L. Methyl jasmonate drai cally enhances the accumulation of phenolic acids in *Salvia miltiorrhiza* hairy root cultures. *Physiol. Plant* **2009**, *137*, 1−9.

(10) Xiao, Y.; Gao, S. H.; Di, P.; Chen, J. F.; Chen, W. S.; Zhang, L. Lithospermic acid B is more responsive to silver ions (Ag^+) than rosmarinic acid in *Salvia miltiorrhiza* hairy root cultures. *Biosci. Rep.* **2009**, *30*, 33−40.

(11) Lee, C. Y.; Agrawal, D. C; Wang, C. S.; Yu, S. M.; Chen, J. J.; Tsay, H. S. T-DNA activation tagging as a tool to isolate *Salvia miltiorrhiza* transgenic lines for higher yields of tanshinones. *Planta Med.* **2008**, *74*, 780−786.

(12) Hu, P.; Luo, G.; Zhao, Z.; Jiang, Z. Quality assessment of Radix *Salviae Miltiorrhizae*. *Chem. Pharm. Bull.* (*Tokyo*) **2005**, *53*, 481−486.

(13) Petersen, M.; Simmonds, M. S. Rosmarinic acid. *Phytochemistry* **2003**, *62*, 121−125.

(14) Boudet, A. M. Evolution and current status of research in phenolic compounds. *Phytochemistry* **2007**, *68*, 2722−2735.

(15) Winkel-Shirley, B. Flavonoid biosynthesis. A colorful model for genetics, biochemistry, cell biology, and biotechnology. *Plant Physiol.* **2001**, *126*, 485−493.

(16) Ferrer, J. L.; Austin, M. B.; Stewart, C. J.; Noel, J. P. Structure and function of enzymes involved in the biosynthesis of phenylpropanoids. *Plant Physiol. Biochem.* **2008**, *46*, 356−370.

(17) Butelli, E.; Titta, L.; Giorgio, M.; Mock, H. P.; Matros, A.; Peterek, S.; Schijlen, E. G.; Hall, R. D.; Bovy, A. G.; Luo, J.; Martin, C. Enrichment of tomato fruit with health-promoting anthocyanins by expression of select transcription factors. *Nat. Biotechnol.* **2008**, *26* (11), 1301−1308.

(18) Bovy, A.; de Vos, R.; Kemper, M.; Schijlen, E.; Pertejo, A. M.; Muir, S.; Collins, G.; Robinson, S.; Verhoeyen, M.; Hughes, S.; Santos-Buelga, C; van Tunen, A. High-flavonol toma-toes resulting from the heterologous expression of the maize transcription factor genes *LC* and *Cl*. *Plant Cell* **2002**, *14*, 2509−2526.

(19) Borevitz, J. O.; Xia, Y. J.; Blount, J.; Dixon, R. A.; Lamb, C. Activation tagging identifies a conserved MYB regulator of phenylpropanoid biosynthesis. *Plant Cell* **2000**, *12*, 2383−2393.

(20) Zhou, L. L.; Zeng, H. N.; Shi, M. Z.; Xie, D. Y. Development of tobacco callus cultures over expressing *Arabidopsis PAP1*/*MYB75* transcription factor and characterization of anthocyanin biosynthesis. *Planta* **2008**, *229* (1), 37−51.

(21) Li, X.; Gao, M. J.; Pan, H. Y; Cui, D. J.; Gruber, M. Y. Purple canola: *Arabidopsis PAP1* increases antioxidants and phenolics in *Brassica napus* leaves. *J. Agric. Food Chem.* **2010**, *55*, 1639−1645.

(22) Yan, Y. P.; Wang, Z. Z. Genetic transformation of the medicinal plant *Salvia miltiorrhiza* by *Agrobacterium tumefaciens-mediated* method. *Plant Cell, Tissue Organ Cult*. **2007**, *88*, 175−184.

(23) Yan, Y. P.; Wang, Z. Z.; Tian, W.; Dong, Z. M.; Spencer, D. F. Generation and analysis of expressed sequence tags from the medicinal plant *Salvia miltiorrhiza*. *Sci. China Life Sci*. **2010**, *53*, 273−285.

(24) Song, J.; Wang, Z. Z. RNAi-mediated suppression of the phenylalanine ammonia-lyase gene in *Salvia miltiorrhiza* causes abnormal phenotypes and a reduction in rosmarinic acid biosyn-thesis. *J. Plant Res*. **2010**, in press.

(25) Ma, Q. H. Characterization of a cinnamoyl-CoA reductase that is associated with stem development in wheat. *J. Exp. Bot*. **2007**, *55*, 2011−2021.

(26) Robinson, A. R.; Mansfield, S. D. Rapid analysis of poplar lignin monomer composition by a streamlined thioacidolysis procedure and near-infrared reflectance-based prediction modeling. *Plant J*. **2009**, *55*, 706−714.

(27) Hoffmann, L.; Besseau, S.; Geoffrey, P.; Ritzenthaler, C.; Meyer, D.; Lapierre, C.; Pollet, B.; Legranda, M. Silencing of hydroxycinnamoyl-coenzyme A shikimate/quinate hydroxycin-namoyltransferase affects phenylpropanoid biosynthesis. *Plant Cell* **2004**, *16*, 1446−1465.

(28) Zhang, Y.; Wang, Z. Z. Phenolic composition and antioxidant activities of two *Phlomis* species: A correlation study. *C. R. Biol*. **2009**, *332*, 816−826.

(29) Mano, H.; Ogasawara, F.; Sato, K.; Higo, H.; Minobe, Y. Isolation of a regulatory gene of anthocyanin biosynthesis in tuberous roots of purple-fleshed sweet potato. *Plant Physiol*. **2007**, *143*, 1252−1268.

(30) Omoto, T.; Murakami, Y.; Shimomura, K.; Yoshihira, K.; Mori, K.; Nakashima, T.; Tanaka, M.; Ishimaru, K. Caffeic acid derivatives in Lamiaceae and Boraginaceae plants. *Jpn. J. Food Chem*. **1997**, *4*, 11−16.

Received for review August 20, 2010. Revised manuscript received October 15, 2010. Accepted October 22, 2010. This work benefited from financial support from the National Natural Science Foundation of China (Grant No. 31000134) and the "Foundation for Excellent Doctor Degree Dissertation" of Shaanxi Normal University (S2008YB04), Shaanxi, People's Republic of China.